Organ-Specific Requirements for Thyroid Hormone Receptor Ensure Temporal Coordination of Tissue-Specific Transformations and Completion of *Xenopus* Metamorphosis

Yuki Shibata, Luan Wen,* Morihiro Okada, and Yun-Bo Shi

Background: Thyroid hormone (triiodothyronine [T3]) is essential for the development throughout vertebrates. Anuran metamorphosis mimics mammalian postembryonic development, a period around birth when plasma T3 level peaks and many organs/tissues mature into their adult forms. Compared with the uterus-enclosed mammalian embryos, tadpoles can be easily manipulated to study the roles of T3 and T3 receptors (TRs) in tissue remodeling and adult organ development. We and others have previously knocked out *TRα* or *TRβ* in the diploid anuran *Xenopus tropicalis* and reported distinct effects of the two receptor knockouts on metamorphosis. However, animals lacking either TRα or TRβ can complete metamorphosis and develop into reproductive adults.

Methods: We have generated *TRα* and *TRβ* double knockout animals and carried out molecular and morphological analyses to determine if TR is required for *Xenopus* development.

Results: We found that the *TR* double knockout tadpoles do not respond to T3, supporting the view that there are no other *TR* genes in *X. tropicalis* and that TR is essential for mediating the effects of T3 *in vivo*. Surprisingly, the double knockout tadpoles are able to initiate metamorphosis and accomplish many metamorphic changes, such as limb development. However, all double knockout tadpoles stall and eventually die at stage 61, the climax of metamorphosis, before tail resorption takes place. Analyses of the knockout tadpoles at stage 61 revealed various developmental abnormalities, including precocious ossification and extra vertebrae.

Conclusions: Our data indicate that TRs are not required for the initiation of metamorphosis but is essential for the completion of metamorphosis. Furthermore, the differential effects of *TR* knockout on different organs/tissues suggest tissue-specific roles for TR to control temporal coordination and progression of metamorphosis in various organs.

Keywords: *Xenopus tropicalis*, *Xenopus laevis*, thyroid hormone receptor, transcriptional regulation, amphibian metamorphosis

Introduction

ANURAN METAMORPHOSIS IS the most dramatic morphological transformation that is controlled by thyroid hormone (triiodothyronine [T3]) during vertebrate development. This process mimics postembryonic development in mammals, a period around birth when T3 level also peaks and many organs/tissues mature into their adult forms (1,2). Anuran metamorphosis, however, offers several major advantages for studying the role of T3 and the underlying mechanism in the formation/maturation of the adult organs during postembryonic development, most noticeably the easiness to manipulate this process without any maternal influence.

Earlier transgenic studies in the anuran *Xenopus laevis* have shown that T3 receptors (TRs) are both necessary and sufficient to mediate the causative effects of T3 on amphibian metamorphosis (3). Like all other vertebrates, there are two types of TRs, TRα and TRβ, in both the pseudotetraploid *X. laevis* and the highly related but diploid species *Xenopus tropicalis* (4,5). These receptors are nuclear transcription factors that can repress or activate T3-inducible genes in the presence or absence

Section on Molecular Morphogenesis, National Institute of Child Health and Human Development, National Institutes of Health, Bethesda, Maryland.
*Current address: Shenzhen Key Laboratory of Synthetic Genomics and Center for Synthetic Genomics, Institute of Synthetic Biology, Shenzhen Institutes of Advanced Technology, Chinese Academy of Sciences, Shenzhen, China.

of T3, respectively, even in the context of chromatin (2,6–11). These molecular properties and the expression profiles of the $TR\alpha$ and $TR\beta$ genes have led to the proposal of a dual function model for TRs during *X. laevis* development (12,13). According to the dual function model, during premetamorphosis when plasma T3 level is low or absent, TR is mainly unliganded and functions to repress the expression of T3-inducible genes to prevent precocious metamorphosis. When T3 becomes available, T3 binds to TR and liganded TR in turn activates the target genes to induce metamorphosis. Over the years, studies from different laboratories have provided strong molecular and transgenic evidence to support this model (3,13–27). However, the pseudotetraploid nature of the *X. laevis* genome and the lack of good technologies to inactivate the endogenous genes had long prevented the analysis of function of the endogenous *TR* genes during *X. laevis* development.

With the advent of gene editing technologies that are applicable to amphibians, we and others have begun to investigate the role of endogenous TRs by using the diploid anuran *X. tropicalis*, which is highly related to *X. laevis*, especially with regard to metamorphosis (4,28–32). Both $TR\alpha$ and $TR\beta$ have been knocked out individually, and analyses of the single knockout animals have revealed interesting but distinct phenotypes (33–42). Knocking out $TR\alpha$ leads to derepression of T3-inducible genes in premetamorphic tadpoles and premature initiation of metamorphosis, as reflected by limb morphogenesis, and also decreased response to exogenous T3 and reduced rate of metamorphic progression during natural metamorphosis (33,34,37–41). However, it has no detectable effect on tail resorption with overall time from fertilization to the completion of metamorphosis similar between wild-type (WT) and knockout animals. However, knocking out $TR\beta$ has little effect on premetamorphic development and limb metamorphosis but delays tail resorption (35,36,42). Interestingly, both $TR\alpha$ and $TR\beta$ individual knockout animals can complete metamorphosis with no apparently morphological defects in the resulting froglets, raising an interesting question whether TR is required for metamorphosis, especially considering that inactivating both $TR\alpha$ and $TR\beta$ does not impair mouse embryonic development (43,44).

In this study, we have knocked out the *X. tropicalis* $TR\beta$ gene by using clustered regularly interspaced short palindromic repeats (CRISPR)/Cas9 genome editing technology in $TR\alpha$-knockout animals and generated homozygous *TR*-null ($TR\alpha^{(-/-)}TR\beta^{(-/-)}$) animals. Our analyses of the WT and knockout animals show that T3 target gene expression was derepressed in $TR\alpha^{(-/-)}TR\beta^{(-/-)}$ premetamorphic tadpoles, and such tadpoles were completely resistant to T3 treatment. Developmentally, homozygous *TR* double knockout led to tadpole lethality at stage 61, the climax of metamorphosis, with little tail resorption and gill repression taking place. Examination of the tadpoles at stage 61 revealed various developmental abnormalities in the *TR* double knockout (TRDKO) animals, which include precocious ossification. Analysis of keratin gene expression in the back skin revealed that TRDKO prevented the repression of larval keratin gene expression normally occurring at stage 61 without affecting the activation of adult keratin gene expression. Our data suggest that TR is not required for the initiation of metamorphosis but is essential for the temporal coordination of the transformation of different organs to ensure the completion of metamorphosis via

repression of T3 target genes during premetamorphosis and activation of these genes when bound by T3.

Materials and Methods

Experimental animals

WT adult *X. tropicalis* were purchased from Nasco. Embryos and tadpoles were staged according to the study by Nieuwkoop and Faber (45). $TR\alpha$ mutation frog ($TR\alpha^{(+/-)}TR\beta^{(+/+)}$ and $TR\alpha^{(-/-)}TR\beta^{(+/+)}$) was generated and reared in the 9-L plastic container (37,38). All animal care and treatments were performed as approved by the Animal Use and Care Committee of the Eunice Kennedy Shriver National Institute of Child Health and Human Development.

Generation of TRβ-knockout X. tropicalis *animals by using CRISPR-Cas9, genome editing technology and genotyping*

CRISPR-short guide RNA (sgRNA) was designed, as described (46), to target exon 2 of the $TR\beta$ gene, upstream of the DNA binding domain (Supplementary Table S1 and Fig. 1). CRISPR-sgRNA-injected embryos generated from mating of $TR\alpha^{(+/-)}TR\beta^{(+/+)}$ and $TR\alpha^{(+/+)}TR\beta^{(+/+)}$ animals were reared to sexual maturity (F0-generation frogs). A sexually mature F0 frog was mated with a $TR\alpha^{(-/-)}TR\beta^{(+/+)}$ frog, and their offspring were screened to identify $TR\alpha$ homozygous and $TR\beta$ heterozygous mutant tadpoles ($TR\alpha^{(-/-)}TR\beta^{(+/-)}$). After $TR\alpha^{(-/-)}TR\beta^{(+/-)}$ mutants were sexually mature (F1 frogs), female and male mutant frogs were primed with 20 U of human chorionic gonadotropin (Novarel), one day before egg laying. They were then boosted with another injection of 200 U of human chorionic gonadotropin on the second day for natural mating to obtain the *TR* total knockout ($TR\alpha^{(-/-)}TR\beta^{(-/-)}$) animals (F2 generation). The resulting fertilized eggs/embryos were collected and reared for 3–4 days at 25°C to reach the onset feeding stage (stage 45). The tadpoles were then transferred to a 4-L container and fed.

Tadpoles were anesthetized with MS222 for photography, tail clipping, and body length measurement. For genotyping, the tadpole tail tip (about 5 mm or less) was clipped and lysed in 20 μL QuickExtract DNA extraction solution (Epicentre) at 65°C for 20 minutes. After incubating at 95°C for five minutes, 1 μL of the DNA extraction solution was immediately used for genotyping by polymerase chain reaction (PCR). For the F1 animals, genotyping was performed with PCR amplification of the $TR\alpha$-transcriptional activator–like effector nuclease (TALEN)-targeted (37,38) and $TR\beta$-CRISPR-targeted regions (Supplementary Table S1). This led to the identification of F1 animals with a homozygous mutation for $TR\alpha$ and out-of-frame mutations for $TR\beta$. A 19 base out-of-frame deletion $TR\beta$ line (Fig. 1) was chosen for further studies. Genotyping the offspring of this F1 line for $TR\alpha$ was subsequently performed by PCR as described (38). $TR\beta$ mutants were identified by PCR with the forward primer 1, 5′-TCAATGGAACCCTTTGGAGCTG-3′ and the reverse primer 1, 5′-ACAGTTACAGGCATTTCCAGGC-3′ for 35 cycles of 94°C for 10 seconds, 60°C for 5 seconds, and 72°C for 45 seconds. The PCR products were analyzed by gel electrophoresis and purified by using QIAGEN PCR purification kit (Qiagen), followed by sequencing (Eurofins genomics). For the F2 generation, the genotyping of $TR\beta$ was
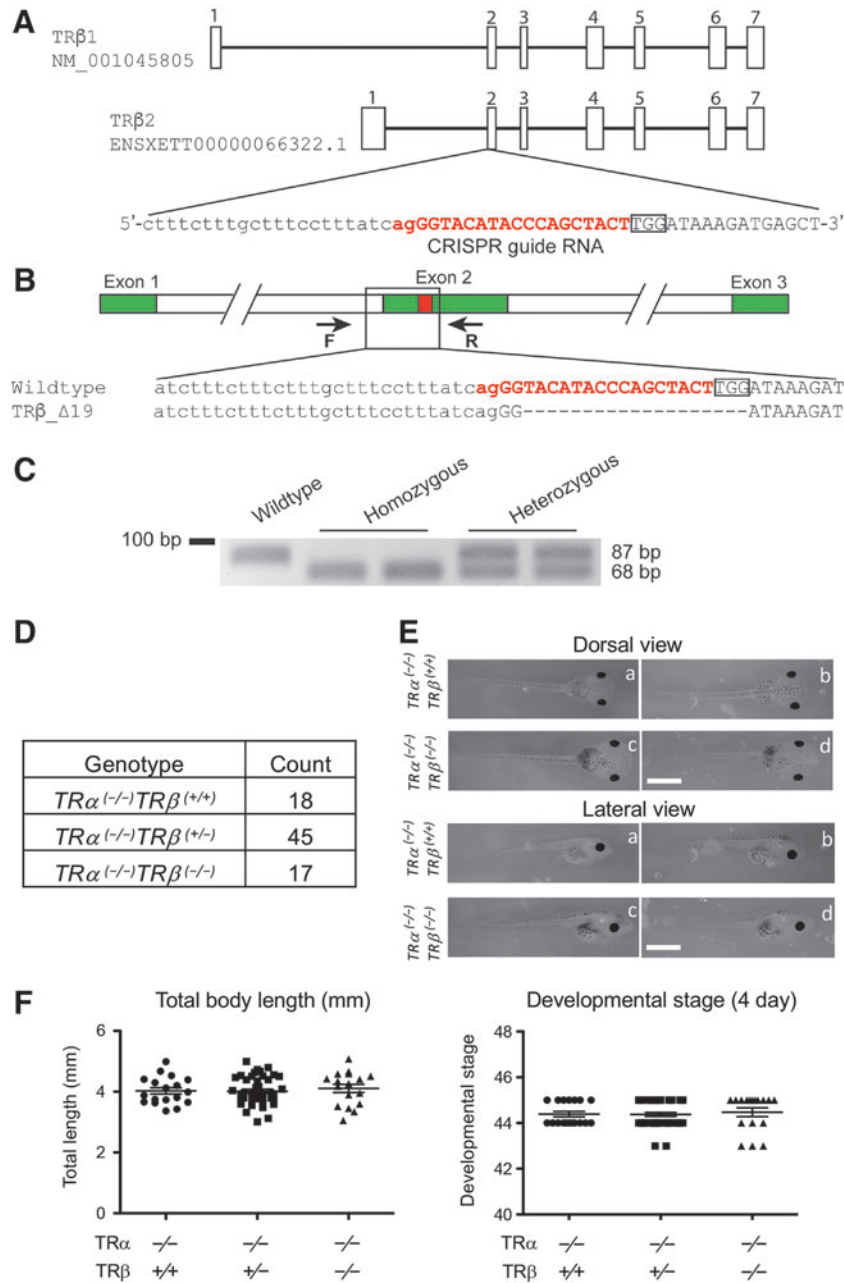
A

TRβ1
NM_001045805

1　2 3　4 5　6 7

TRβ2
ENSXETT00000066322.1

1　2 3　4 5　6 7

5'-ctttctttgctttcctttatc**agGGTACATACCCAGCTACT**TGGATAAAGATGAGCT-3'
CRISPR guide RNA

B

Exon 1　Exon 2　Exon 3

F　R

Wildtype　atctttctttctttgctttcctttatc**agGGTACATACCCAGCTACT**TGGATAAAGAT
TRβ_Δ19　atctttctttctttgctttcctttatcag**GG**--------------------ATAAAGAT

C

100 bp

Wildtype　Homozygous　Heterozygous

87 bp
68 bp

D

Genotype	Count
TRα (-/-)TRβ (+/+)	18
TRα (-/-)TRβ (+/-)	45
TRα (-/-)TRβ (-/-)	17

E

Dorsal view

TRα (-/-) TRβ (+/+)　a　b
TRα (-/-) TRβ (-/-)　c　d

Lateral view

TRα (-/-) TRβ (+/+)　a　b
TRα (-/-) TRβ (-/-)　c　d

F

Total body length (mm)

Developmental stage (4 day)

TRα　-/-　-/-　-/-
TRβ　+/+　+/-　-/-

TRα　-/-　-/-　-/-
TRβ　+/+　+/-　-/-

FIG. 1. Knocking out both *TR* genes does not affect *Xenopus tropicalis* embryogenesis. (**A**) Genomic structure of the *X. tropicalis TRβ* gene and the CRISPR-sgRNA against *X. tropicalis TRβ*. There are two known transcripts for *X. tropicalis TRβ*, each with seven exons (boxes). The *TRβ*-specific sgRNA was designed to target exon 2, and the sgRNA sequences are shown in red. (**B**) Schematic diagram depicting the sequence of the sgRNA-targeted region in the WT and a *TRβ*-mutant (19 bases deletion) animals. Arrows represent primers used for genotyping: the forward primer F and the reverse primer R, respectively. (**C**) Representative examples of genotyping by PCR. Genotyping PCR was carried out on genomic DNA by using a common primer set, primer F and primer R. The presence of only upper (105 bp) or lower (86 bp) band in the gel indicates a WT or homozygous mutant animal, respectively, while the presence of both upper and lower band indicates a heterozygous mutant. (**D**) Mendelian distribution of four-day-old tadpoles from mating of two *TRα* (-/-)*TRβ* (+/-) animals. Genotyping PCR was carried out by using tail tip genomic DNA of four-day-old tadpoles, which were at stage 45/46, the onset of tadpole feeding, and the result was close to the expected Mendelian ratio. (**E**) Representative photos of four-day-old tadpoles of the WT or homozygous *TRβ*-knockout genotype in the homozygous *TRα* mutant background. The upper column is the dorsal view and the lower column is the lateral view. Lowercase letters in both columns indicate the same tadpole. Note that no obvious difference was present between the WT or homozygous *TRβ* tadpoles in the homozygous *TRα* mutant background. Scale bars: 1 mm. (**F**) Knocking out *TRβ* in the homozygous *TRα* mutant background does not affect the body length and developmental stage of four-day-old tadpoles. The data are shown as the mean, marked as a line, and SE. No significant difference was observed in both parameters for the three genotypes, indicating that removing *TRβ* has no effect on *X. tropicalis* embryogenesis. CRISPR, clustered regularly interspaced short palindromic repeats; PCR, polymerase chain reaction; SE, standard error; sgRNA, short guide RNA; T3, thyroid hormone; TR, T3 receptor; WT, wild type.

performed by PCR with the forward primer 2, 5′-GGACA ACATTAGATCTTTCTTTCTTTG-3′ and the reverse primer 2, 5′-CACACCACGCATAGCTCATC-3′ for 33 cycles of 94°C for 30 seconds, 60°C for 30 seconds, and 72°C for 20 seconds. The PCR products were analyzed by gel electrophoresis.

T3 treatment

Randomly selected stage 54 tadpoles were treated with 10 nM T3 for 18 hours at 25°C. The tadpole tail tip (about 5 mm or less) was cut for genotyping, and the rest of each animal was frozen in liquid nitrogen. The frozen tadpoles of the same genotype were combined together for RNA extraction. For the long-term T3 treatment, 17–27 tadpoles of different genotypes at stage 54 were pooled together in 4-L plastic container and treated with or without 5 nM T3 for five days at 25°C.

RNA extraction and quantitative real-time PCR

Total RNA of the intestine, tail, or limb was extracted with RNeasy® Mini Kit 250 (Qiagen) according to the manufacturer's instructions. The homogenates of individual tissues from at least five animals, or five whole animals, of each genotype were combined together for RNA extraction. The RNA concentration was measured by using a NanoDrop (Thermo Scientific). The same amount of RNA from each of the three genotypes (TRβ: WT, heterozygous, and homozygous) was reverse-transcribed with the QuantiTect Reverse Transcription Kit (Qiagen). The cDNA was analyzed by quantitative real-time PCR by using the SYBR Green method. The PCR primers for the internal control genes $ef1\alpha$ and $rpl8$ were described previously (37,38) (note that $ef1\alpha$ and $rpl8$ mRNA expression was similar in all genotypes; data not shown). All expression data were normalized against that of the internal control gene $ef1\alpha$ or $rpl8$. The expression analyses were performed at least twice, with similar results. The primer sequences are listed in Supplementary Tables S1 and S2.

Staining for ossification

Whole mount staining was carried out according to the study by Inouye (47), with slight modifications. In brief, tadpoles at stages 54–66 were fixed in 4% paraformaldehyde/phosphate-buffered saline for one day at 4°C. After dehydration with 95% ethanol for four days, the specimens were deskinned and eviscerated and then delipidated with acetone for one day. The specimens were stained in 0.015% Alcian blue 8GS (Sigma)–0.005% Alizarin red S (Acros Organics), 5% acetic acid, and 70% ethanol at 37°C for one day. The stained specimens were put stepwise into 30% saturated borate–0.5% Trypsin (Sigma) at 37°C for one day, 1% KOH and 20% glycerol for one day, and 50%, 80% glycerol for two hours. The cleared specimens were stored in 100% glycerol. The cartilage was then stained blue, and the calcified bone stained red.

Statistical analysis

Data are presented as mean ± standard error. The significance of differences between groups was evaluated by one-way analysis of variance followed by Bonferroni multiple comparison test or Student's t-test using Prism 5 (GraphPad Software).

Results

Generation of X. tropicalis TR total knockout animals via genome editing

To investigate the role of endogenous TRs during vertebrate development, we adapted the genome editing technologies to knockout both TR genes in $X.$ tropicalis. We previously generated $TR\alpha$-knockout animals by using TALEN technology. To generate TRDKO animals, we used CRISPR technology to generate mosaic $TR\beta$-knockdown frogs (F0) (46). First, we designed a CRISPR guide RNA targeting in exon 2, which encodes part of the DNA binding domain, of $X.$ tropicalis $TR\beta$ (Fig. 1A). Then, we microinjected the mRNAs encoding the CRISPR sgRNA and Cas9 into one-cell stage embryos generated from a $TR\alpha$ heterozygous frog ($TR\alpha^{(+/-)}TR\beta^{(+/+)}$) and a WT frog ($TR\alpha^{(+/+)}TR\beta^{(+/+)}$). The resulting F0 animals had mosaic mutations in the target region of the $TR\beta$ gene. We raised some of these F0 animals of the $TR\alpha^{(+/-)}TR\beta^{mosaic}$ genotype to sexual maturity and then crossed them with $TR\alpha$ homozygous knockout animals ($TR\alpha^{(-/-)}TR\beta^{(+/+)}$) to generate F1, $TR\beta$ heterozygous animals ($TR\alpha^{(-/-)}TR\beta^{(+/-)}$). We selected one heterozygous mutant line with a 19 base out-of-frame deletion in the target region of $TR\beta$ gene for further analysis (Fig. 1B). We finally produced $TR\beta$ homozygous knockout F2 generation animals (TRDKO, $TR\alpha^{(-/-)}TR\beta^{(-/-)}$) by intercrossing the F1 frogs and confirmed genotype by PCR (Fig. 1C).

TR is not required for frog embryogenesis

To analyze the effects of TR knockout on embryogenesis, we measured the body length and determined the developmental stage of individual animals according to their external morphology four days after fertilization (45). Genotyping of 80 F2 siblings from mating two $TR\alpha^{(-/-)}TR\beta^{(+/-)}$ animals revealed a Mendelian distribution of the three expected genotypes (Fig. 1D). Furthermore, there was no significant difference in body length or developmental stage among the three genotypes: $TR\alpha^{(-/-)}TR\beta^{(+/+)}$, $TR\alpha^{(-/-)}TR\beta^{(+/-)}$, and $TR\alpha^{(-/-)}TR\beta^{(-/-)}$ (Fig. 1E, F) and all animals reached stage 45, the onset of feeding. These results indicate that removing TRβ in the $TR\alpha$ knockout background had no effect on embryogenesis. In addition, earlier studies have shown that TRα single knockout also had no detectable gross developmental defects on embryogenesis (38). Thus, TR is not essential for $Xenopus$ embryogenesis.

TRβ represses T3 target genes in premetamorphic tadpoles and upregulates them in the presence of exogenous T3 to facilitate precocious tissue transformations in premetamorphic tadpoles

To investigate the effect of $TR\beta$ knockout on premetamorphic tadpoles in the absence of TRα, we first measured the age in days for the animals to reach stage 54, commonly considered to be the onset of metamorphosis. Eighty F2 siblings as generated above were randomly selected when individual tadpoles reached stage 54 based on morphology (Fig. 2A), and their ages were recorded (Fig. 2B). After measuring the total body length, snout-vent length and
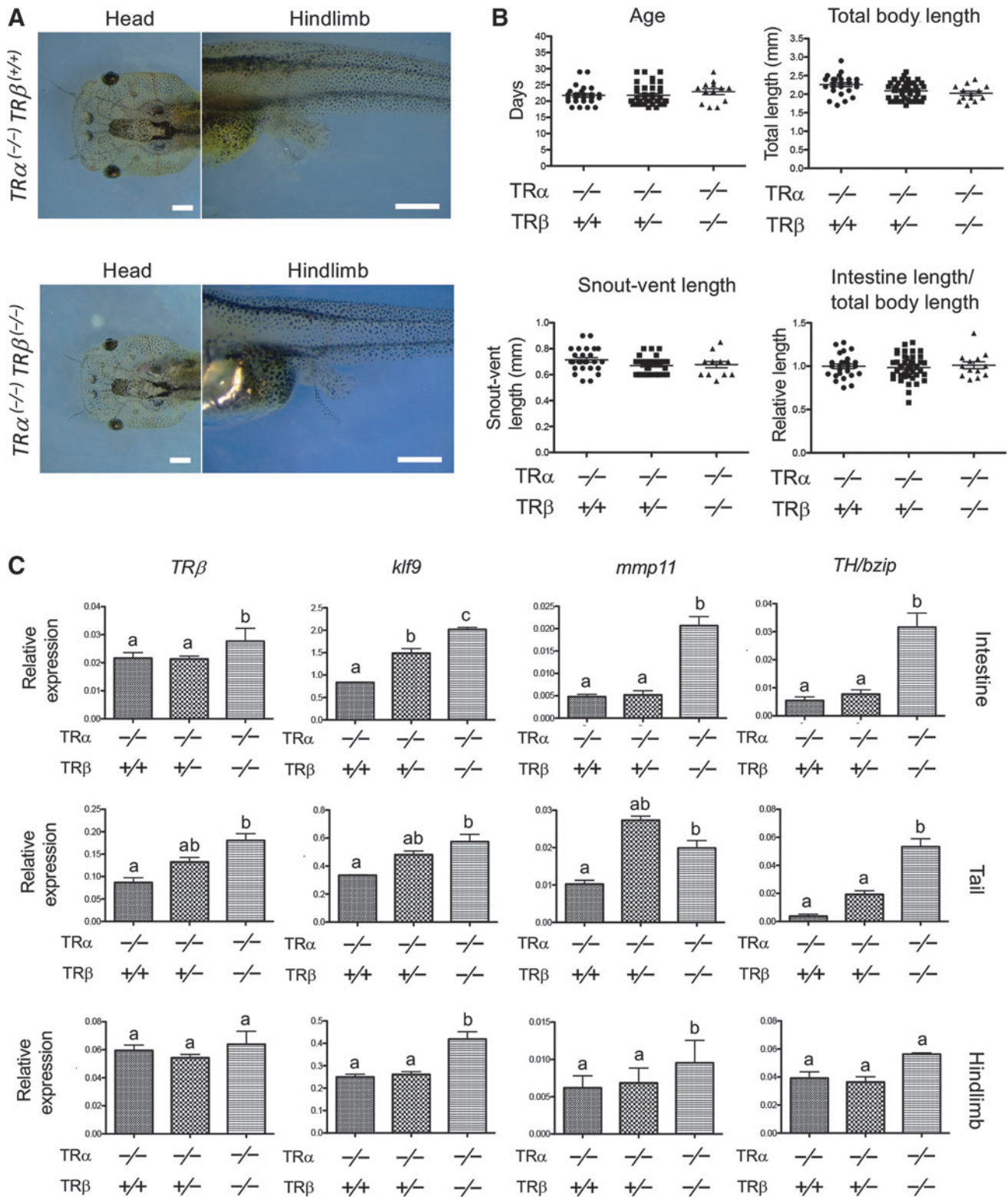
FIG. 2. Knocking out *TRβ* in the homozygous *TRα* mutant background derepresses the expression of T3-inducible genes in premetamorphic tadpoles with little effect on premetamorphic development. (**A**) Representative photos of tadpoles at stage 54. Note that the *TRα* $^{(-/-)}$*TRβ* $^{(+/+)}$ and *TRα* $^{(-/-)}$*TRβ* $^{(-/-)}$ tadpoles at stage 54 have a similar head (dorsal view) and hind limb morphology (lateral view). Scale bars: 1 mm. (**B**) *TRα* $^{(-/-)}$*TRβ* $^{(+/+)}$ and *TRα* $^{(-/-)}$*TRβ* $^{(-/-)}$ tadpoles have similar developmental rates (age, days to stage 54), total body length, snout-vent length, and intestinal length (normalized against the total body length) at stage 54. These results are plotted as the mean, marked as a line, and SE. (**C**) Increased basal expression of known T3 target genes due to *TRβ* knockout in premetamorphic tadpoles. Total RNA from three different organs, intestine, tail, and hind limb, of stage 54 tadpoles of the three genotypes, was used for qRT-PCR analysis of the expression of four well-known T3 direct target genes: *TRβ*, *klf9*, *mmp11*, and *TH/bzip*. The expression levels were normalized against that of *ef1α*. Different lowercase letters denote statistically significant differences ($p < 0.05$). qRT-PCR, quantitative real-time PCR.

intestine length, the genotype of each tadpole was determined by PCR, showing the presence of 26 $TR\alpha^{(-/-)}TR\beta^{(+/+)}$, 41 $TR\alpha^{(-/-)}TR\beta^{(+/-)}$, and 13 $TR\alpha^{(-/-)}TR\beta^{(-/-)}$ tadpoles among them (Fig. 2B). Interestingly, no difference was observed for any of the four parameters among the three genotypes (Fig. 2B), suggesting that $TR\beta$ knockout in the background of $TR\alpha$ knockout does not affect premetamorphic tadpole development.

We next investigated the expression of several known direct T3 target genes, $TR\beta$ (48), $klf9$ (49), $mmp11$ (50), and $TH/bzip$ (51) in three different organs: intestine, tail, and hind limb of premetamorphic tadpoles. The results show that the expression of all these genes was increased in $TR\alpha^{(-/-)}TR\beta^{(-/-)}$ tadpoles, although few changes were observed in most cases in $TR\alpha^{(-/-)}TR\beta^{(+/-)}$ heterozygous animals (Fig. 2C). Thus, in the absence of TRα, TRβ repressed the expression of the target genes in premetamorphic tadpoles.

To investigate whether TRβ can activate target gene expression in the absence of endogenous TRα and if gene activation by T3 requires any TR, we treated stage 54 premetamorphic tadpoles containing all three genotypes together with or without 5 nM T3 for five days, a long-term treatment known to induce external morphological changes in WT tadpoles. As shown in Figure 3A, $TR\alpha^{(-/-)}TR\beta^{(+/+)}$ tadpoles had most dramatic responses to T3 treatment, with obvious gill resorption, reshaping of the head to a pointy structure, and hind limb development (Fig. 3A). However, the double knockout ($TR\alpha^{(-/-)}TR\beta^{(-/-)}$) tadpoles had little noticeable changes, while the $TR\beta$ heterozygous ($TR\alpha^{(-/-)}TR\beta^{(+/-)}$) animals were in between (Fig. 3A). Quantitative measurement of the lengths of the intestine and hind limbs, normalized against the total body length, showed that the T3-induced changes were essentially abolished in the TRDKO tadpoles (Fig. 3B).

Molecularly, we found that T3 was able to induce the expression of target genes, such as $TR\beta$, $klf9$, $mmp11$, and $TH/bzip$, in the intestine, tail, and hind limb of $TR\beta$ WT ($TR\alpha^{(-/-)}TR\beta^{(+/+)}$) and heterozygous ($TR\alpha^{(-/-)}TR\beta^{(+/-)}$) animals even in the absence of TRα (Fig. 3C). In contrast, the fold induction by T3 was close to 1 for most of the genes in different organs in TRDKO ($TR\alpha^{(-/-)}TR\beta^{(-/-)}$) tadpoles (Fig. 3C). It is interesting to note that the fold induction by T3
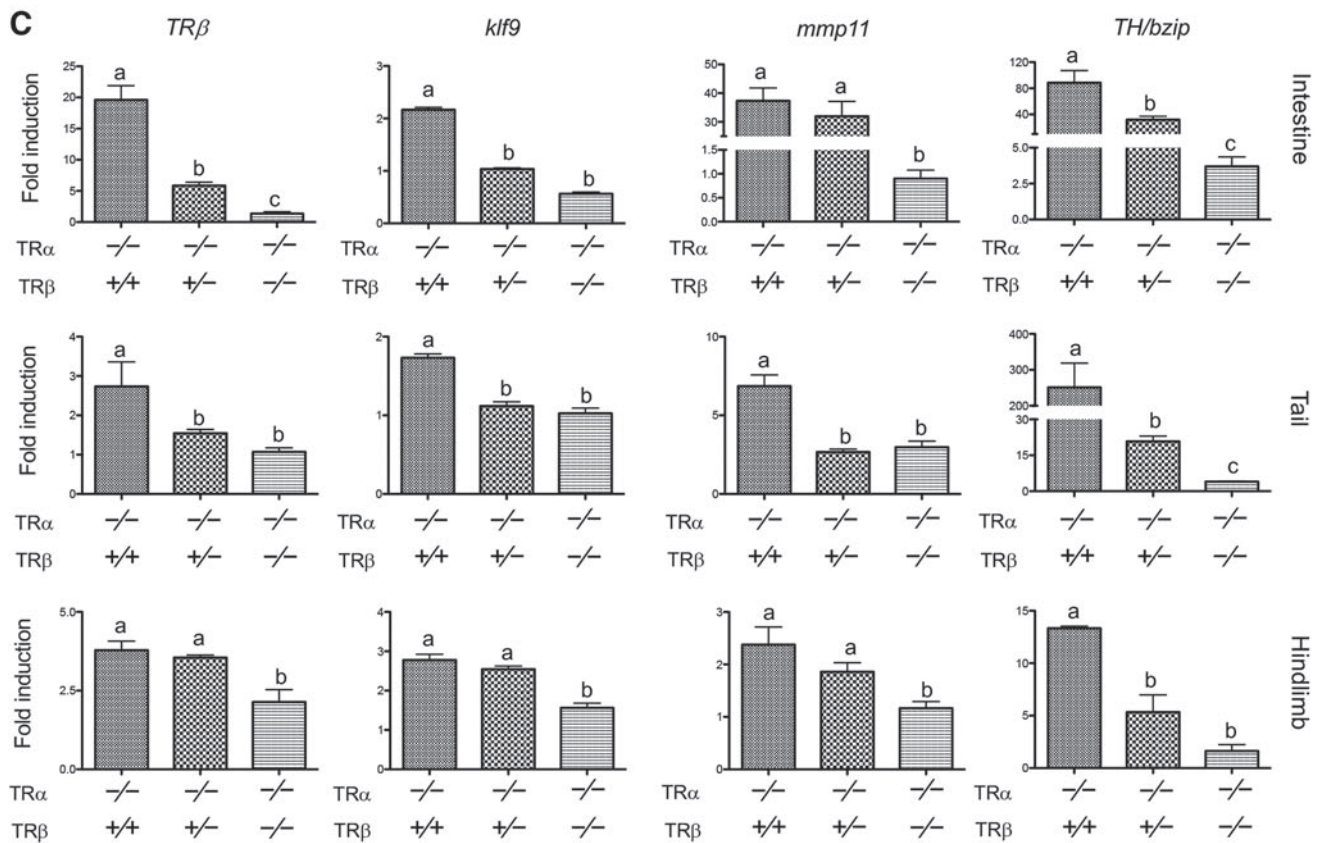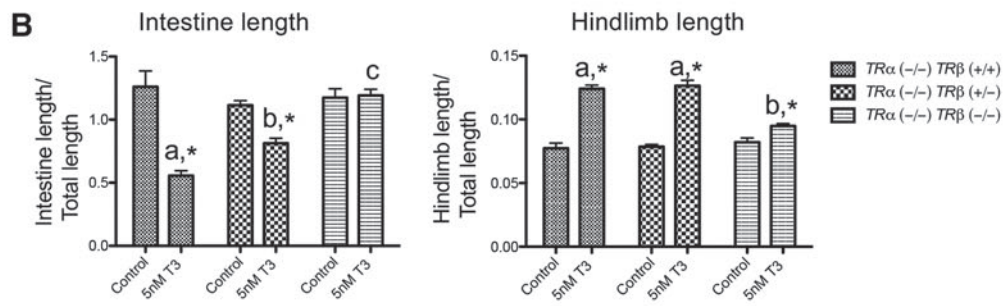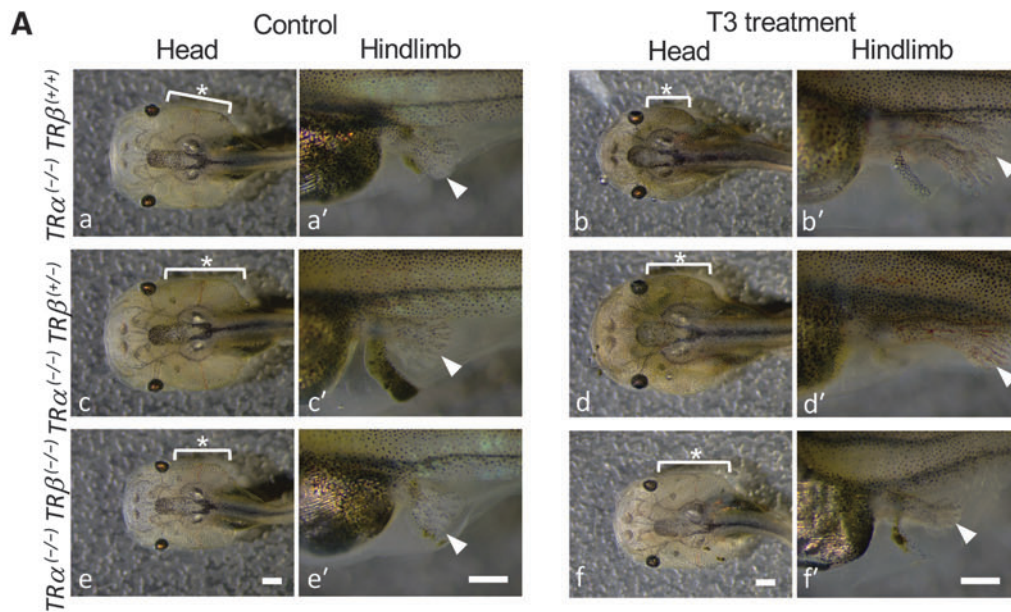
was above 1 for some genes in some organs in the TRDKO tadpoles, for example, $TH/bzip$ in the intestine and $TR\beta$ in the hind limb (Fig. 3C). This small residual effect is likely due to nongenomic action of T3, although it had no detectable effect on tadpole development (Fig. 3B). In addition, earlier transgenic studies with dominant negative and dominant positive TRs have shown that T3 signaling via TRs is both necessary and sufficient for $Xenopus$ metamorphosis, suggesting that nongenomic action of T3 is not required for $Xenopus$ development (14,16,17). Thus, our results suggest that the endogenous TRα and TRβ are responsible for mediating gene activation and metamorphic effects of T3 in $X. tropicalis$.

Complete TR knockout is lethal at climax of metamorphosis

Having shown that $TR\beta$ knockout in the TRα knockout background did not affect premetamorphic tadpole development, we next investigated whether TR double knockout tadpoles could undergo metamorphosis. We reared F2 siblings from mating of $TR\alpha^{(-/-)}TR\beta^{(+/-)}$ heterozygous frogs together and found that all animals were able to develop beyond stage 54, suggesting that all could initiate metamorphosis. We recorded the body length and age of each animal when it reached stage 58, the stage of forelimb emergence and onset of metamorphic climax (Fig. 4A) (45), and genotyped the animal. We found that in the TRα knockout background, $TR\beta$ knockout slightly reduced the body length of the tadpoles at stage 58 (Fig. 4B) and also slowed the tadpole development to stage 58 (Fig. 4C). There were no significant differences in either parameter between the $TR\beta$ WT and heterozygous knockout tadpoles.

When individual tadpoles at stage 58 were allowed to develop further to stage 61, the climax stage when the lengths of the nervus olfactorius (NO) and bulbus olfactorius (BO) are the same (45), we found that the TRDKO tadpoles took twice as long (10 days vs. 5 days) to develop from stage 58 to stage 61 compared with the $TR\beta$ WT and heterozygous knockout tadpoles (Fig. 4D). Furthermore, we observed that TRDKO tadpoles remained at stage 61 for 1–2 weeks (data not shown) and died before reaching stage 62, while all tadpoles of the other two genotypes developed to stage 62 as

FIG. 3. Knocking out $TR\beta$ in the homozygous TRα mutant background abolishes tadpole response to exogenous T3. (**A**) Representative photos of tadpoles treated with 5 nM T3 for five days. Age-matched stage 54 tadpoles were randomly collected and kept in a 4-L plastic container. They were genotyped after treatment with (**b, d, f**) or without (**a, c, e**) 5 nM T3 for five days and photographed dorsally (**a–f**) or laterally (**a′–f′**). Note that after T3 treatment, $TR\alpha^{(-/-)}TR\beta^{(+/+)}$ tadpoles (**b**) were morphologically distinct from $TR\alpha^{(-/-)}TR\beta^{(-/-)}$ tadpoles (**f**). The former have pointy heads and more developed hind limbs, while the latter are similar to those without T3 treatment (**e**). The $TR\beta$ heterozygous tadpoles (**d**) show a morphologically intermediate phenotype. Lowercase letter in the panels indicates the same tadpoles. Asterisks (*) indicate the position of the gills. Arrowheads: hind limb. Scale bars: 1 mm. (**B**) TRDKO tadpoles show little or no response to T3. The lengths of the intestine and hind limb of the tadpoles treated with or without T3 as in (**A**) were measured and normalized against the total body length. Note that after T3 treatment, the intestine is significantly shortened, while the hind limbs are larger except in the $TR\alpha^{(-/-)}TR\beta^{(-/-)}$ tadpoles, which show essentially no response to T3 (although a very small increase in hind limb length was observed). No significant difference was observed in both parameters for the three genotypes in the absence of T3. Different lowercase letters denote statistically significant differences ($p < 0.01$), and asterisks (*) indicate a significant difference when compared with the control group without T3 treatment ($p < 0.01$). (**C**) T3 treatment fails to induce target gene expression in TRDKO tadpoles. Age-matched tadpoles at stage 54 were treated with 10 nM T3 for 18 hours. The expression of several known T3 target genes, $TR\beta$, $klf9$, $mmp11$, and $TH/bzip$, was analyzed by qRT-PCR in the intestine, tail, and hind limb, respectively, and the expression levels were normalized against that of $ef1\alpha$. The results are shown as fold-induction in response to T3. Note that in the double knockout tadpoles, the fold induction was about 1 for all genes in all organs, that is, there was no T3 response. Different lowercase letters denote statistically significant differences ($p < 0.05$). TRDKO, TR double knockout.
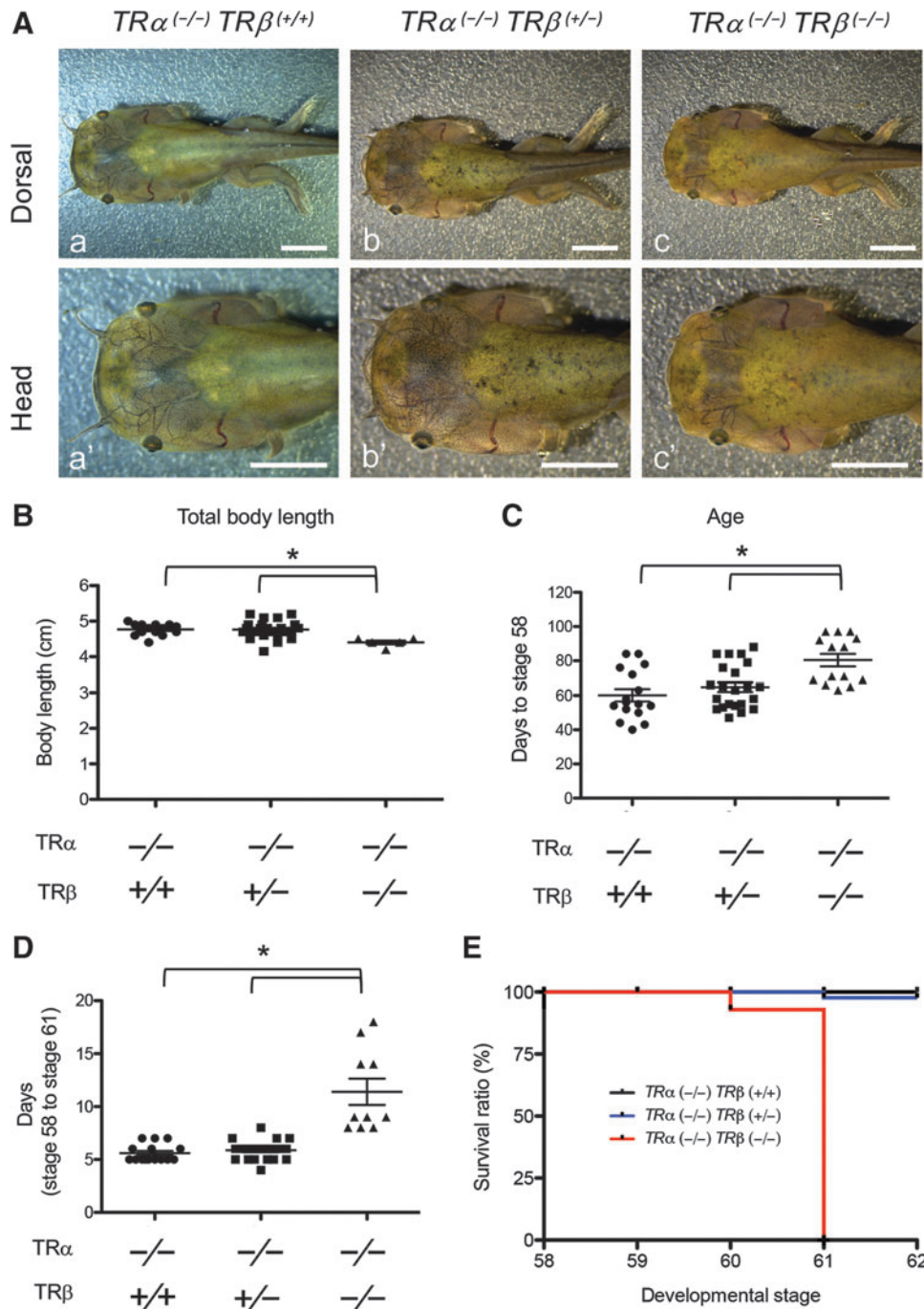
A

Control — Head, Hindlimb; T3 treatment — Head, Hindlimb

$TR\alpha^{(-/-)} TR\beta^{(+/+)}$ (a, a', b, b')
$TR\alpha^{(-/-)} TR\beta^{(+/-)}$ (c, c', d, d')
$TR\alpha^{(-/-)} TR\beta^{(-/-)}$ (e, e', f, f')

B

Intestine length — Intestine length/Total length

Hindlimb length — Hindlimb length/Total length

$TR\alpha (-/-) TR\beta (+/+)$
$TR\alpha (-/-) TR\beta (+/-)$
$TR\alpha (-/-) TR\beta (-/-)$

C

$TR\beta$, *klf9*, *mmp11*, *TH/bzip* — Intestine, Tail, Hindlimb

FIG. 4. Total knockout of *TRs* reduces the rate of natural metamorphic progression and causes tadpoles lethality at the climax of metamorphosis. (**A**) Representative photos of tadpoles for three *TRβ* genotypes at the stage of forelimb emergence (stage 58). Adult $TR\alpha^{(-/-)}TR\beta^{(+/-)}$ animals were mated, and the resulting tadpoles were euthanized when their forelimbs broke through the membrane-enclosure, photographed, and genotyped to identify the three genotypes [(**a**) $TR\alpha^{(-/-)}TR\beta^{(+/+)}$, (**b**) $TR\alpha^{(-/-)}TR\beta^{(+/-)}$, and (**c**) $TR\alpha^{(-/-)}TR\beta^{(-/-)}$]. Lowercase letters indicate the same tadpole with two different views: dorsal view (upper) and a higher magnification from the dorsal side for the head (lower: **a′–c′**). Scale bars: 5 mm. (**B**) TRDKO tadpoles have shorter body length at the onset of metamorphic climax (stage 58). The body length of individual tadpoles at stage 58 as identified in (**A**) was measured and plotted with the mean, marked as a line, and SE. The asterisks (*) indicate a significant difference for the three genotypes ($p < 0.01$). (**C**) TRDKO tadpoles have delayed onset of metamorphic climax (stage 58). The age of individual tadpoles at stage 58 as identified in (**A**) was recorded and plotted with the mean, marked as a line, and SE. The asterisks (*) indicate a significant difference for the three genotypes ($p < 0.01$). (**D**) TRDKO tadpoles have a reduced rate of metamorphic progression at the climax stages. The time in days for the tadpoles as identified in (**A**) to go from stage 58 to stage 61 [as judged by the length of NO and BO. At stage 61, NO = BO (Fig. 6A)] was recorded and plotted with the mean, marked as a line, and SE. The asterisks (*) indicate a significant difference for the three genotypes ($p < 0.01$). (**E**) TRDKO leads to lethality at metamorphic climax. The tadpoles as identified in (**A**) were allowed to develop from stage 58 or stage 62, or when they died and were then genotyped. The survival rate for each of the three genotypes, $TR\alpha^{(-/-)}TR\beta^{(+/+)}$ ($n = 17$), $TR\alpha^{(-/-)}TR\beta^{(+/-)}$ ($n = 21$), and $TR\alpha^{(-/-)}TR\beta^{(-/-)}$ ($n = 15$), was determined and plotted. Note that no double knockout tadpoles developed to stage 62. BO, bulbus olfactorius; NO, nervus olfactorius.

expected (Fig. 4E). Thus, in the absence of TRα, TRβ knockout not only delays metamorphic progression but also leads to tadpole lethality at the climax of metamorphosis, indicating that TR is essential for anuran metamorphosis.

Complete TR *knockout alters and/or accelerates some metamorphic events while preventing others*

The above results indicate that TR is not required for initiation of metamorphosis and progression up to stage 61. However, all TRDKO tadpoles died at stage 61. This lethal phenotype may be due to the failure of one or more tissues to undergo proper metamorphic progression or mis-coordination of temporal progressions in different organs/tissues. To determine the developmental defects due to total *TR* knockout, we next focused on stage 61 tadpoles of two genotypes: total *TR* knockout (*TRα* $^{(-/-)}$*TRβ* $^{(-/-)}$) and *TR* WT (*TRα* $^{(+/+)}$*TRβ* $^{(+/+)}$). Total *TR* knockout tadpoles had normal forelimbs and hind limbs but an abnormal head structure (Fig. 5A, also see below). Interestingly, Alizarin red (for

ossification) and Alcian blue (for cartilages) whole mount staining revealed more advanced bone development in the *TR*-knockout tadpoles, such as advanced maxilla and nasal ossification in cranial bone (red color: Fig. 5B-a′, a″, b′, and b″). Additionally, in WT animals, there are nine vertebrae and their ossification occurs gradually during metamorphosis, with the vertebra IX (sacral vertebra) fused to the illium by stage 65/66 (Supplementary Fig. S1). The hypochord begins to ossify around stage 61 and the process ends after metamorphosis (Supplementary Fig. S2). The TRDKO tadpoles at stage 61 had several additional ossified vertebrae at the body–tail junction and appeared to have completed hypochord ossification and developed a sacral vertebra structure fused with vertebra VIII (Fig. 5B-a‴, a⁗, b‴, and b⁗) (52). In WT animals at the end of metamorphosis, the hypochord comes into contact with the anterior end of the coccyx to form the urostyle (Supplementary Fig. S1) (53). Unexpectedly, longer vertebra bones (arrowheads in Fig. 5B-b, b‴, and b⁗) were found in the *TR*-knockout tadpoles at stage 61 (Supplementary Fig. S1) (53).
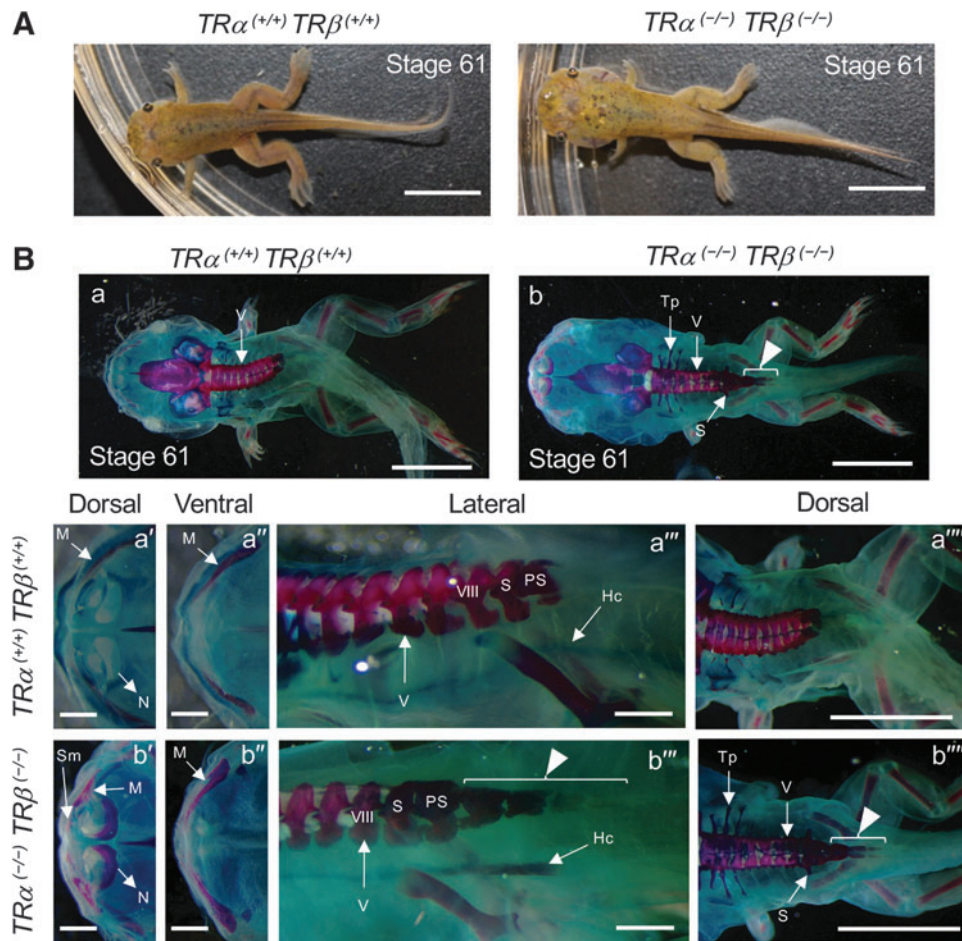

FIG. 5. Total knockout of *TRs* alters skeletal development and ossification at the climax of metamorphosis. (**A**) Representative photos of a WT (*TRα* $^{(+/+)}$*TRβ* $^{(+/+)}$) (left panel) and *TRα* $^{(-/-)}$*TRβ* $^{(-/-)}$ (right panel) tadpoles at stage 61. The tadpoles were allowed to develop to stage 61 regardless of age and were then photographed. Scale bars: 5 mm. (**B**) *TRα* $^{(-/-)}$*TRβ* $^{(-/-)}$ tadpoles have increased ossification and additional ossified vertebrae at the end of the body at stage 61. Alizarin red (for ossification) and Alcian blue (for cartilages) whole mount staining of tadpoles at stage 61. (**a**) *TRα* $^{(+/+)}$*TRβ* $^{(+/+)}$ and (**b**) *TRα* $^{(-/-)}$*TRβ* $^{(-/-)}$. (**a′, b′**) are dorsal views and (**a″, b″**) are ventral views of high magnification of the mouth region. (**a‴, b‴**) High magnification of the body. Note the increased ossification in the head region and extra ossified vertebrae (arrow heads in **b‴, b⁗**) at the body–tail junction. Scale bars: 1 cm (**a, a′, b, b′**), 1 mm (**a″, a‴, b″, b‴**), 5 mm (**a⁗, b⁗**). Hc, hypochord; M, maxilla; N, nasal; PS, postsacral vertebra; S, sacral vertebra; Sm, septomaxilla; Tp, transverse process; V, vertebra; VIII, eighth vertebra.

Developmentally, we observed that these abnormalities were present as early as stage 58 in the TRDKO animals (Supplementary Figs. S1 and S2). Thus, removal of TR leads to precocious ossification and abnormal vertebra development.

As indicated above (Fig. 5A), at stage 61, when the lengths of the NO and the BO are equal (Fig. 5A) (45), TRDKO animals have an abnormal head structure and their gills appeared to be largely intact until the animals eventually died (Fig. 5; data not shown). To analyze this further, we determined the ratio of the width at the gill position (Fig. 6A, black line) to the width at the eye position (Fig. 6A, white lines), as well as the head area (Fig. 6A, the region within the yellow rectangle) by using the Image J Software. The results show that TRDKO tadpoles at stage 61 have a larger ratio of the two widths (Fig. 6B) and a larger head area (Fig. 6C) compared with those in WT stage 61 tadpoles. These were consistent with the obviously larger gill areas in the knockout tadpoles (Fig. 6A), indicating that TR is required for gill resorption.

Next, we analyzed the transformation of the skin, which involves the transition from the expression of larval keratin (xlk) in tadpoles to the expression of adult keratins (xak-b and xak-c) during/after metamorphosis (54,55). We determined the expression of *keratin* genes in WT tadpoles at stages 54, 61, and 66 and in TRDKO tadpoles at stages 54 and 61. As expected, in WT tadpoles, *xlk* expression was reduced by stage 61 and completely repressed by the end of metamorphosis (Fig. 6D). In contrast, both adult keratin genes were not expressed in premetamorphic WT tadpoles but activated by stage 61 and remained highly expressed in post-metamorphic frogs (Fig. 6D). Interestingly, in the TRDKO tadpoles at stage 61, no repression of the larval *keratin* gene was observed, while both adult *keratin* genes were activated (Fig. 6D), suggesting that TRDKO prevents the degeneration of larval keratinocytes but allows the development of adult keratinocytes.

Discussion

Since the discovery over a century ago that frog metamorphosis could be accelerated by feeding tadpoles with thyroid (56,57), anurans have been used as a model to study vertebrate development, particularly the role of hormones. This has contributed to the discovery of T3 and the study of the role of T3 during vertebrate development. Earlier studies, particularly in *X. laevis*, have led to a dual function model for TRs during frog development, but the roles of endogenous TRs have been investigated only more recently with the development of gene editing technologies and the use of the diploid anuran *X. tropicalis*. Individual *TRα* and *TRβ* knockout studies have indeed demonstrated critical and distinct involvement of the two TRs in metamorphosis (33–42). However, neither TRα nor TRβ appears to be essential for anuran metamorphosis as individual knockout animals complete metamorphosis with no obvious morphological defects, although the overall developmental rate is affected. Our double knockout studies shown here demonstrate unambiguously that TRs are essential for anuran metamorphosis and reveal broad roles of both unliganded and liganded TR in coordinating the development of different organs/tissues to ensure normal tadpole development and survival of the animal through metamorphosis.

TRα and TRβ are the only receptors mediating gene regulation by T3 in X. tropicalis

Studies on T3-inducible promoters *in vitro* and in cell cultures have shown that TRs can bind to T3 response elements constitutively to activate the promoters in the presence and repress them in the absence of T3, respectively. Consistent with this, *TRα* knockout in *X. tropicalis* leads to up-regulation of known T3-inducible genes in premetamorphic tadpoles when little T3 is present and most or all the receptors are likely unliganded (37–39). Our results here show that disrupting *TRβ* in the *TRα* knockout background further increases the expression of these T3-inducible genes in premetamorphic tadpoles, suggesting that both receptors participate in the repression of target genes when T3 is not available. Similarly, T3 treatment of premetamorphic tadpoles shows that *TRα* knockout reduces the induction of these genes by T3 (37–39), and additional knockout of *TRβ* completely abolishes the induction of these genes by T3 (Fig. 3). Thus, there are no other nuclear receptors for T3 in *X. tropicalis*, and all developmental effects of T3 are mediated by TRα and TRβ.

Diverse metamorphic changes in many organs do not require TR

TRDKO tadpoles can develop up to stage 61, indicating that TRs are not required for many of the metamorphic transformations. There are three types of tissue transformations during metamorphosis: adult organ development, larval organ resorption, and organ remodeling. Both adult organ development and organ remodeling take place for at least some organs in TRDKO tadpoles. The most dramatic is limb development, which is essentially complete by stage 61 and does not require TR. Among the organs undergoing remodeling, the development of the bones, including vertebrae and jaw, takes place and appears even more advanced in TRDKO tadpoles at stage 61 compared with that in the WT animals. The remodeling of the head, leading to a more pointed structure, also occurs without TR. In addition, adult *keratin* genes are activated in the TRDKO tadpoles at stage 61, just like in WT animals (Fig. 6), suggesting that the development of the adult skin can occur in the absence of TR. While the exact cause of these TR-independent metamorphic changes remains to be determined, it is very likely that the removal of TR leads to derepression of T3-inducible genes, which in turn facilitates metamorphosis. Thus, unliganded TRs are critical to maintain normal tadpole development and prevent premature metamorphosis in different organs/tissues.

TRDKO inhibits metamorphic changes in most organs and causes abnormal development and lethality at climax of metamorphosis

While many metamorphic processes can occur without TRs, many others require TR-mediating T3 signaling. Most notably, there are two tadpole-specific organs, the tail and gills, which are completely resorbed by the end of metamorphosis. The gills are mostly resorbed in the WT tadpoles by stage 61. However, little gill resorption occurs in stage 61 TRDKO tadpoles (Figs. 5 and 6). In addition, tail resorption takes place mostly from stage 62 on. All knockout tadpoles are developmentally stalled at stage 61 and die before tail
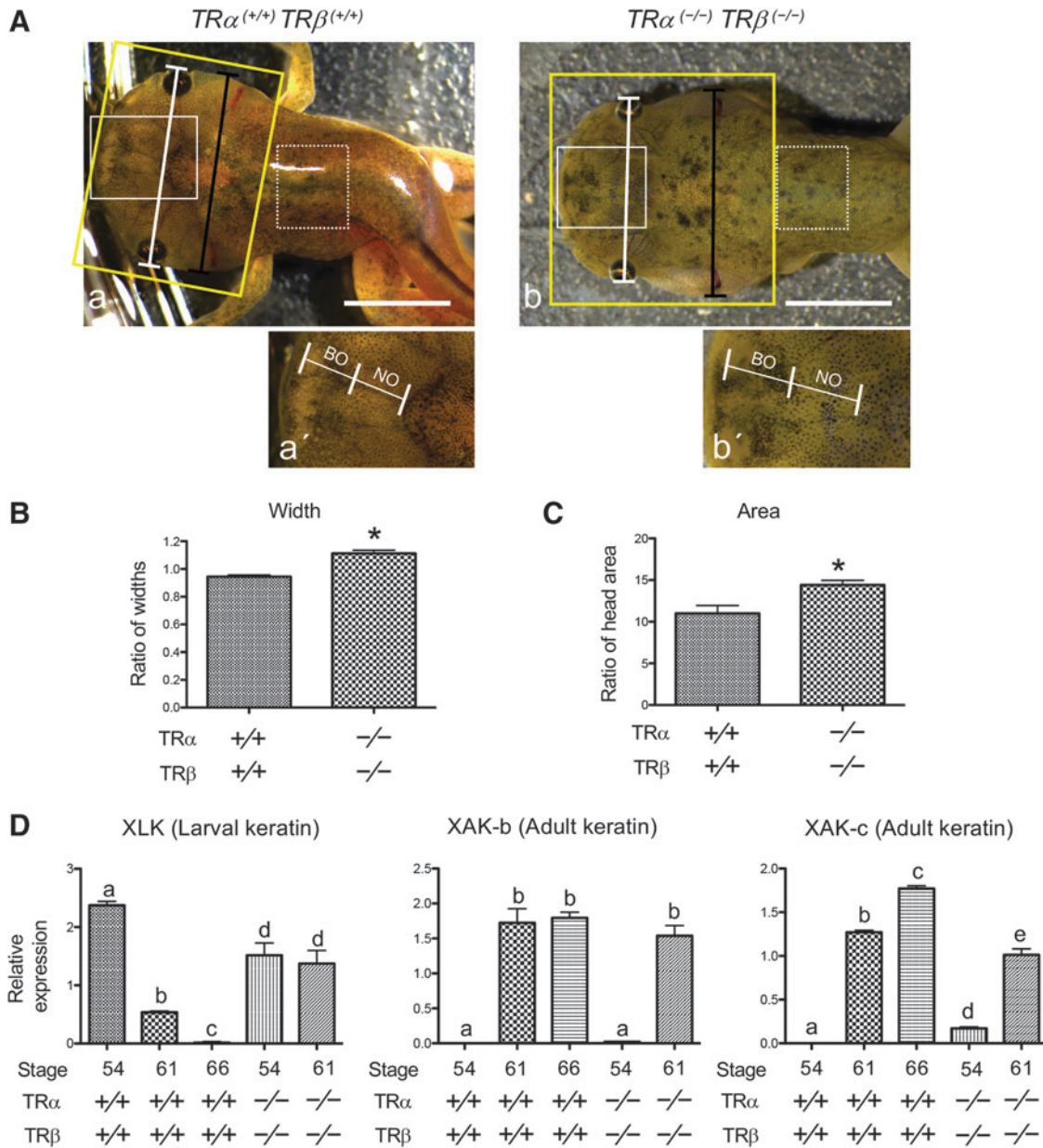
FIG. 6. TR is required for larval tissue resorption. **(A)** Representative photos of the heads of $TR\alpha^{(+/+)}TR\beta^{(+/+)}$ and $TR\alpha^{(-/-)}TR\beta^{(-/-)}$ tadpoles at stage 61, the climax of metamorphosis. The developmental stage was determined based on the length of the NO and BO with NO = BO at stage 61 (note that the boundaries of NO and BO could be easily determined based on morphological differences by microscopy). **(a)** $TR\alpha^{(+/+)}TR\beta^{(+/+)}$ and **(b)** $TR\alpha^{(-/-)}TR\beta^{(-/-)}$. The black line in the top panel spans the width from the outer edge of the gills, and the white line spans the width from the outer edge of the eyes. The yellow box encloses the head region. Higher magnification of areas boxed with white lines in **(a, b)** is shown in **(a′, b′)**. An area of the dorsal skin used for gene expression studies in D is shown in the dashed box. Scale bars: 5 mm. **(B)** TRDKO inhibits gill repression at the metamorphic climax. The ratio of the width at the gill position [black line in the top panel of **(A)**] to the width at the eye position [white line in the top panel of **(A)**] was calculated as a measure of the relative gill size. Data are expressed as mean plus SE ($TR\alpha^{(+/+)}TR\beta^{(+/+)}$ [$n=9$] and $TR\alpha^{(-/-)}TR\beta^{(-/-)}$ [$n=6$]). The asterisk (*) indicates a significant difference when compared with that for $TR\alpha^{(+/+)}TR\beta^{(+/+)}$ ($p < 0.01$). **(C)** TRDKO inhibits the reduction in head size associated with jaw remodeling and gill resorption. The head area, enclosed by yellow box in the top panel of **(A)**, was measured by the ImageJ software and is presented as mean plus SE ($TR\alpha^{(+/+)}TR\beta^{(+/+)}$ [$n=9$] and $TR\alpha^{(-/-)}TR\beta^{(-/-)}$ [$n=6$]). The asterisk (*) indicates a significant difference when compared with that for $TR\alpha^{(+/+)}TR\beta^{(+/+)}$ ($p < 0.01$). **(D)** TRDKO blocks the downregulation of larval *keratin* genes but allows the expression of adult *keratin* genes at the metamorphic climax. The dorsal skin, as shown in the area enclosed by dashed boxes in A, of the WT ($TR\alpha^{(+/+)}TR\beta^{(+/+)}$) at stages 54, 61, and 66, and TRDKO ($TR\alpha^{(-/-)}TR\beta^{(-/-)}$) tadpoles stages 54 and 61 were dissected for total RNA extraction and qRT-PCR analysis of the expression of a larval skin marker, *larval keratin (xlk)*, and two adult skin markers, adult *keratins b and c (xak-b and xak-c)*. The qRT-PCR for all genes and on all samples was performed simultaneously. The expression levels were normalized against that of *rpl8*. The groups included 5, 3, 3 WT ($TR\alpha^{(+/+)}TR\beta^{(+/+)}$) tadpoles at stage 54, 61, and 66; and 5 $TR\beta$ homozygous ($TR\alpha^{(-/-)}TR\beta^{(-/-)}$) tadpoles each at stages 54 and 61, respectively. Note that, as expected, the larval *keratin* gene was repressed by stage 61, while adult *keratin* genes were upregulated by stage 61 in WT animals. Interestingly, in the double knockout animals at stage 61, no repression of the larval *keratin* gene was observed, although the adult *keratin* genes were activated as in the WT animals. Different lowercase letters denote statistically significant differences ($p < 0.05$).

resorption, suggesting that larval organ resorption requires T3 action through TRs. In addition, in the body skin, while the adult skin appears to form as reflected by the expression of adult *keratin* genes in the TRDKO tadpoles at stage 61, the larval *keratin* gene is not suppressed at stage 61 in the TRDKO animals, in contrast to that observed in the WT tadpoles (Fig. 6), suggesting that larval keratinocyte death is inhibited or delayed in the absence of TR. Thus, TR appears to be required for larval cell death in many, if not all, organs during metamorphosis.

The *TR* double knock phenotypes that we observed bear similarities to those of *TR*-knockout mice. Mice with the knockout of either *TRα* or *TRβ* knockout can develop into adulthood, although with various abnormalities (58–60). Similarly, double knockout mice for both *TRα* and *TRβ* knocked out are born alive (43,44,61). Interestingly, two studies found that the double knockout mice developed into adults (44,61), while another found that the double knockout mice stopped growing and eventually died around five weeks of age (43). This latter phenotype is similar to what we have observed here for the double knockout tadpoles. While the exact cause for the different findings in mouse is unclear, it has been suggested that different knockout strategies may have different effects on the truncated TRα isoforms derived from a promoter located in the intron 7 of the *TRα* gene, consequently leading to different outcomes (61). It remains to be determined if such TRα isoforms exist in *X. tropicalis* and contribute to tadpole lethality that we have observed for the TRDKO tadpoles.

Our study also reveals that removal of TRs leads to accelerated endochondral ossification in the skull and the notochord, and additional vertebra formation by stage 58, if not earlier (Fig. 5B and Supplementary Fig. S2) during early metamorphosis when plasma T3 levels are still relatively low (45). This suggests that unliganded TRs not only temporally control the timing of endochondral ossification but are also important for spatial development of the vertebrae. Similarly, T3 and TRs are critical for normal endochondral ossification and bone development in mice (44,61–64). *TRα* single or TRDKO mice have impaired bone development and lower ossification (43,44,61), and a dominant negative *TRα*-knockin mutation in heterozygous mice causes dwarfism and delayed endochondral and intramembranous ossification (65). However, the dominant negative knockin mutation in the *TRβ* locus leads to advanced endochondral and intramembranous ossification in homozygous mice, accompanied by very high levels of circulating T3 (65,66). These findings suggest that unliganded TRs also inhibit ossification during mouse development. It is tempting to speculate that TRs have conserved roles in regulated temporal coordination of tissue remodeling and adult organ maturation during postembryonic development.

In summary, the findings shown here reveal broad roles of TRs that are essential for tadpole development and survival through anuran metamorphosis. TRDKO affects diverse processes during *Xenopus* development. Embryogenesis is the only developmental period with no obvious alterations due to *TR* knockout. It has been shown earlier that *TRα* knockout leads to premature initiation of metamorphosis (i.e., reaching stage 54 at younger age) (33–39), and TRDKO tadpoles behave similarly as *TRα*-knockout animals in this respect (Fig. 2), indicating that unliganded TR, mainly TRα, controls metamorphic timing. During the first half of metamorphosis (from onset at stage 54 to the early climax at stage 58), TR controls the rate of metamorphic progression, with *TRα* knockout dramatically slowing down this process (33,34,37–39) and additional *TRβ* knockout further reducing the developmental rate (Fig. 4C). During the second half of metamorphosis (stage 58–stage 66), *TRα* knockout has little effect (33,34,37–39) while *TRβ* knockout delays this process (35,36). TRDKO tadpoles also delay their development from stage 58 onward and stall at stage 61 before eventual death (Fig. 4D, E). The ability of double knockout animals to reach stage 61 strongly suggests that the removal of the repression caused by unliganded TRs in tadpoles is sufficient for many metamorphic events to take place. The metamorphic lethal phenotype at stage 61 caused by TRDKO, however, is likely due to the incomplete and/or uncoordinated transformations of many organs due to the lack of T3 signaling by liganded TRs. Thus, anuran metamorphosis involves sophisticated spatiotemporal coordination of the transformation of different organs by employing both unliganded and T3-bound TRs via the control of T3 availability. The unliganded TRs prevent precocious metamorphosis in different organs by repressing T3-inducible genes. With the rising concentration of plasma T3, T3-inducible genes are first derepressed and then further activated to even higher levels. The ability of TRDKO animals to develop to stage 61 suggests that most of the metamorphic changes up to this stage simply require the derepression. The metamorphic changes that fail to occur in the TRDKO animals likely require additional activation beyond derepression. These distinct requirements of T3-TR signaling suggest that a precise regulation of the levels of TR and T3 in different organs is important for metamorphosis. Given all organs are exposed to the same plasma T3 levels, it is very likely that other factors influencing T3 signaling, such as transporters and deiodinases, are involved in this process. Clearly, future studies on this are needed. In addition, in light of the findings reported here, it may also be interesting to determine whether TRDKO in mouse also leads to incomplete maturation of adult organs and/or defects in temporal coordination of adult organ development and to identify the molecular mechanisms underlying these alterations/defects during metamorphosis or postembryonic development in mammals.

Author Disclosure Statement

No competing financial interests exist.

Funding Information

Supplementary Material

Supplementary Table S1
Supplementary Table S2
Supplementary Figure S1
Supplementary Figure S2

References

1. Tata JR 1993 Gene expression during metamorphosis: an ideal model for post-embryonic development. Bioessays **15:**239–248.
2. Shi Y-B 1999 Amphibian Metamorphosis: From Morphology to Molecular Biology. John Wiley & Sons, Inc., New York.
3. Buchholz DR, Paul BD, Fu L, Shi YB 2006 Molecular and developmental analyses of thyroid hormone receptor function in *Xenopus laevis*, the African clawed frog. Gen Comp Endocrinol **145:**1–19.
4. Wang X, Matsuda H, Shi Y-B 2008 Developmental regulation and function of thyroid hormone receptors and 9-cis retinoic acid receptors during *Xenopus tropicalis* metamorphosis. Endocrinology **149:**5610–5618.
5. Yaoita Y, Shi YB, Brown DD 1990 *Xenopus laevis* alpha and beta thyroid hormone receptors. Proc Natl Acad Sci U S A **87:**7090–7094.
6. Wong J, Shi YB, Wolffe AP 1995 A role for nucleosome assembly in both silencing and activation of the Xenopus TR beta A gene by the thyroid hormone receptor. Genes Dev **9:**2696–2711.
7. Lazar MA 1993 Thyroid hormone receptors: multiple forms, multiple possibilities. Endocr Rev **14:**184–193.
8. Yen PM 2001 Physiological and molecular basis of thyroid hormone action. Physiol Rev **81:**1097–1142.
9. Evans RM 1988 The steroid and thyroid hormone receptor superfamily. Science **240:**889–895.
10. Tsai MJ, O'Malley BW 1994 Molecular mechanisms of action of steroid/thyroid receptor superfamily members. Ann Rev Biochem **63:**451–486.
11. Laudet V, Gronemeyer H 2002 The Nuclear Receptor FactsBook. Academic Press, San Diego.
12. Shi Y-B, Wong J, Puzianowska-Kuznicka M, Stolow M 1996 Tadpole competence and tissue-specific temporal regulation of amphibian metamorphosis: roles of thyroid hormone and its receptors. BioEssays **18:**391–399.
13. Sachs LM, Damjanovski S, Jones PL, Li Q, Amano T, Ueda S, Shi YB, Ishizuya-Oka A 2000 Dual functions of thyroid hormone receptors during Xenopus development. Comp Biochem Physiol B Biochem Mol Biol **126:**199–211.
14. Schreiber AM, Das B, Huang H, Marsh-Armstrong N, Brown DD 2001 Diverse developmental programs of *Xenopus laevis* metamorphosis are inhibited by a dominant negative thyroid hormone receptor. Proc Natl Acad Sci U S A **98:**10739–10744.
15. Brown DD, Cai L 2007 Amphibian metamorphosis. Dev Biol **306:**20–33.
16. Buchholz DR, Hsia VS-C, Fu L, Shi Y-B 2003 A dominant negative thyroid hormone receptor blocks amphibian metamorphosis by retaining corepressors at target genes. Mol Cell Biol **23:**6750–6758.
17. Buchholz DR, Tomita A, Fu L, Paul BD, Shi Y-B 2004 Transgenic analysis reveals that thyroid hormone receptor is sufficient to mediate the thyroid hormone signal in frog metamorphosis. Mol Cell Biol **24:**9026–9037.
18. Shi Y-B 2009 Dual functions of thyroid hormone receptors in vertebrate development: the roles of histone-modifying cofactor complexes. Thyroid **19:**987–999.
19. Nakajima K, Yaoita Y 2003 Dual mechanisms governing muscle cell death in tadpole tail during amphibian metamorphosis. Dev Dyn **227:**246–255.
20. Denver RJ, Hu F, Scanlan TS, Furlow JD 2009 Thyroid hormone receptor subtype specificity for hormone-dependent neurogenesis in *Xenopus laevis*. Dev Biol **326:**155–168.
21. Bagamasbad P, Howdeshell KL, Sachs LM, Denver BA, Denver RJ 2008 A role for basic transcription element-binding protein 1 (BTEB1) in the autoinduction of thyroid hormone receptor beta. J Biol Chem **283:**2275–2285.
22. Schreiber AM, Mukhi S, Brown DD 2009 Cell-cell interactions during remodeling of the intestine at metamorphosis in *Xenopus laevis*. Dev Biol **331:**89–98.
23. Shi Y-B 1994 Molecular biology of amphibian metamorphosis: a new approach to an old problem. Trends Endocrinol Metab **5:**14–20.
24. Shi YB, Matsuura K, Fujimoto K, Wen L, Fu L 2012 Thyroid hormone receptor actions on transcription in amphibia: the roles of histone modification and chromatin disruption. Cell Biosci **2:**42.
25. Grimaldi A, Buisine N, Miller T, Shi YB, Sachs LM 2013 Mechanisms of thyroid hormone receptor action during development: lessons from amphibian studies. Biochim Biophys Acta **1830:**3882–3892.
26. Puzianowska-Kuznicka M, Damjanovski S, Shi Y-B 1997 Both thyroid hormone and 9-cis retinoic acid receptors are required to efficiently mediate the effects of thyroid hormone on embryonic development and specific gene regulation in *Xenopus laevis*. Mol Cell Biol **17:**4738–4749.
27. Sachs LM, Shi Y-B 2000 Targeted chromatin binding and histone acetylation in vivo by thyroid hormone receptor during amphibian development. Proc Natl Acad Sci U S A **97:**13138–13143.
28. Bilesimo P, Jolivet P, Alfama G, Buisine N, Le Mevel S, Havis E, Demeneix BA, Sachs LM 2011 Specific histone lysine 4 methylation patterns define TR-binding capacity and differentiate direct T3 responses. Mol Endocrinol **25:**225–237.
29. Amaya E, Offield MF, Grainger RM 1998 Frog genetics: *Xenopus tropicalis* jumps into the future. Trends Genet **14:**253–255.
30. Matsuura K, Fujimoto K, Fu L, Shi Y-B 2012 Liganded thyroid hormone receptor induces nucleosome removal and histone modifications to activate transcription during larval intestinal cell death and adult stem cell development. Endocrinology **153:**961–972.
31. Matsuura K, Fujimoto K, Das B, Fu L, Lu CD, Shi YB 2012 Histone H3K79 methyltransferase Dot1L is directly activated by thyroid hormone receptor during Xenopus metamorphosis. Cell Biosci **2:**25.
32. Sterling J, Fu L, Matsuura K, Shi Y-B 2012 Cytological and morphological analyses reveal distinct features of intestinal development during *Xenopus tropicalis* metamorphosis. PLoS One **7:**e47407.
33. Choi J, Ishizuya-Oka A, Buchholz DR 2017 Growth, development, and intestinal remodeling occurs in the absence of thyroid hormone receptor alpha in tadpoles of *Xenopus tropicalis*. Endocrinology **158:**1623–1633.
34. Choi J, Suzuki KI, Sakuma T, Shewade L, Yamamoto T, Buchholz DR 2015 Unliganded thyroid hormone receptor alpha regulates developmental timing via gene repression as revealed by gene disruption in *Xenopus tropicalis*. Endocrinology **156:**735–744.
35. Sakane Y, Iida M, Hasebe T, Fujii S, Buchholz DR, Ishizuya-Oka A, Yamamoto T, Suzuki KT 2018 Functional analysis of thyroid hormone receptor beta in *Xenopus tropicalis* founders using CRISPR-Cas. Biol Open **7:**pii: bio030338.
36. Nakajima K, Tazawa I, Yaoita Y 2018 Thyroid hormone receptor alpha- and beta-knockout *Xenopus tropicalis*

tadpoles reveal subtype-specific roles during development. Endocrinology **159:**733–743.

37. Wen L, Shi YB 2015 Unliganded thyroid hormone receptor alpha controls developmental timing in *Xenopus tropicalis*. Endocrinology **156:**721–734.

38. Wen L, Shibata Y, Su D, Fu L, Luu N, Shi Y-B 2017 Thyroid hormone receptor α controls developmental timing and regulates the rate and coordination of tissue specific metamorphosis in *Xenopus tropicalis*. Endocrinology **158:** 1985–1998.

39. Wen L, Shi YB 2016 Regulation of growth rate and developmental timing by Xenopus thyroid hormone receptor alpha. Dev Growth Differ **58:**106–115.

40. Sachs LM 2015 Unliganded thyroid hormone receptor function: amphibian metamorphosis got TALENs. Endocrinology **156:**409–410.

41. Yen PM 2015 Unliganded TRs regulate growth and developmental timing during early embryogenesis: evidence for a dual function mechanism of TR action. Cell Biosci **5:**8.

42. Nakajima K, Tazawa I, Shi YB 2019 A unique role of thyroid hormone receptor beta in regulating notochord resorption during Xenopus metamorphosis. Gen Comp Endocrinol **277:**66–72.

43. Gauthier K, Chassande O, Plateroti M, Roux JP, Legrand C, Pain B, Rousset B, Weiss R, Trouillas J, Samarut J 1999 Different functions for the thyroid hormone receptors TRalpha and TRbeta in the control of thyroid hormone production and post-natal development. EMBO J **18:**623–631.

44. Gothe S, Wang Z, Ng L, Kindblom JM, Barros AC, Ohlsson C, Vennstrom B, Forrest D 1999 Mice devoid of all known thyroid hormone receptors are viable but exhibit disorders of the pituitary-thyroid axis, growth, and bone maturation. Genes Dev **13:**1329–1341.

45. Nieuwkoop PD, Faber J 1965 Normal table of *Xenopus laevis*. North Holland Publishing, Amsterdam.

46. Shibata Y, Bao L, Fu L, Shi B, Shi YB 2019 Functional studies of transcriptional cofactors via microinjection-mediated gene editing in Xenopus. Methods Mol Biol **1874:**507–524.

47. Inouye M 1976 Differential staining of cartilage and bone in mouse skeleton by Alcian Blue and Alizarin Red S. Congenit Anom **16:**171–173.

48. Ranjan M, Wong J, Shi YB 1994 Transcriptional repression of Xenopus TR beta gene is mediated by a thyroid hormone response element located near the start site. J Biol Chem **269:**24699–24705.

49. Furlow JD, Kanamori A 2002 The transcription factor basic transcription element-binding protein 1 is a direct thyroid hormone response gene in the frog *Xenopus laevis*. Endocrinol **143:**3295–3305.

50. Fu L, Tomita A, Wang H, Buchholz DR, Shi Y-B 2006 Transcriptional regulation of the *Xenopus laevis* stromelysin-3 gene by thyroid hormone is mediated by a DNA element in the first intron. J Biol Chem **281:**16870–16878.

51. Furlow JD, Brown DD 1999 In vitro and in vivo analysis of the regulation of a transcription factor gene by thyroid hormone during *Xenopus laevis* metamorphosis. Mol Endocrinol **13:**2076–2089.

52. Trueb L, Hanken J 1992 Skeletal development in *Xenopus laevis* (Anura: Pipidae). J Morphol **214:**1–41.

53. Pugener LA, Maglia AM 2009 Skeletal morphogenesis of the vertebral column of the miniature hylid frog *Acris crepitans*, with comments on anomalies. J Morphol **270:** 52–69.

54. Yoshizato K 2007 Molecular mechanism and evolutional significance of epithelial-mesenchymal interactions in the body- and tail-dependent metamorphic transformation of anuran larval skin. Int Rev Cytol **260:**213–260.

55. Watanabe Y, Kobayashi H, Suzuki K, Kotani K, Yoshizato K 2001 New epidermal keratin genes from *Xenopus laevis*: hormonal and regional regulation of their expression during anuran skin metamorphosis. Biochim Biophys Acta **1517:** 339–350.

56. Gudernatch JF 1912 Feeding experiments on tadpoles. I. The influence of specific organs given as food on growth and differentiation: a contribution to the knowledge of organs with internal secretion. Arch Entwicklungsmech Org **35:**457–483.

57. Allen BM 1929 The influence of the thyroid gland and hypophysis upon growth and development of amphibian larvae. Quart Rev Biol **4:**325–352.

58. Forrest D, Erway LC, Ng L, Altschuler R, Curran T 1996 Thyroid hormone receptor beta is essential for development of auditory function. Nat Genet **13:**354–357.

59. Mai W, Janier MF, Allioli N, Quignodon L, Chuzel T, Flamant F, Samarut J 2004 Thyroid hormone receptor alpha is a molecular switch of cardiac function between fetal and postnatal life. Proc Natl Acad Sci U S A **101:**10332–10337.

60. Wikstrom L, Johansson C, Salto C, Barlow C, Barros AC, Baas F, Forrest D, Thoren P, Vennstrom B 1998 Abnormal heart rate and body temperature in mice lacking thyroid hormone receptor. EMBO J **17:**455–461.

61. Gauthier K, Plateroti M, Harvey CB, Williams GR, Weiss RE, Refetoff S, Willott JF, Sundin V, Roux JP, Malaval L, Hara M, Samarut J, Chassande O 2001 Genetic analysis reveals different functions for the products of the thyroid hormone receptor alpha locus. Mol Cell Biol **21:**4748–4760.

62. Kim HY, Mohan S 2013 Role and mechanisms of actions of thyroid hormone on the skeletal development. Bone Res **1:**146–161.

63. Bassett JH, Nordstrom K, Boyde A, Howell PG, Kelly S, Vennstrom B, Williams G R 2007 Thyroid status during skeletal development determines adult bone structure and mineralization. Mol Endocrinol **21:**1893–1904.

64. Bassett JH, Williams GR 2016 Role of thyroid hormones in skeletal development and bone maintenance. Endocr Rev **37:**135–187.

65. O'Shea PJ, Bassett JH, Sriskantharajah S, Ying H, Cheng SY, Williams GR 2005 Contrasting skeletal phenotypes in mice with an identical mutation targeted to thyroid hormone receptor alpha1 or beta. Mol Endocrinol **19:**3045–3059.

66. O'Shea PJ, Harvey CB, Suzuki H, Kaneshige M, Kaneshige K, Cheng SY, Williams GR 2003 A thyrotoxic skeletal phenotype of advanced bone formation in mice with resistance to thyroid hormone. Mol Endocrinol **17:**1410–1424.

Address correspondence to:
Yun-Bo Shi, PhD
Section on Molecular Morphogenesis
National Institute of Child Health
and Human Development
National Institutes of Health
Bethesda, MD 20892

E-mail: shi@helix.nih.gov